UNIVERSITÀ DEGLI STUDI DI PALERMO

Meccanica dei Materiali e delle Strutture
Vol. VI (2016), no.1, pp. 163-170
ISSN: 2035-679X
Dipartimento di Ingegneria Civile, Ambientale, Aerospaziale, Dei Materiali
DICAM

DAMAGE ASSESSMENT OF BRIDGES USING SPATIAL CHARACTERISTICS OF HIGH-RESOLUTION SATELLITE SAR INTENSITY IMAGES

Fumio Yamazaki[*], Kazuki Inoue[†], Wen Liu[*]

[*] Department of Urban Environment Systems, Chiba University
1-33, Yayoi-cyo, Inage-ku, Chiba 263-8522, Japan
e-mail: fumio.yamazaki@faculty.chiba-u.jp, wen.liu@chiba-u.jp

[†]Institute of Industrial Science, The University of Tokyo
4-6-1 Komaba, Meguro-ku, Tokyo 153-8505, Japan.
e-mail: kinoue1994@gmail.com

Key words: Tsunami, TerraSAR-X, Bridge Damage, The 2011 Tohoku Earthquake.

Abstract. *Synthetic Aperture Radar (SAR) sensors onboard satellites are suitable for information gathering in emergency response since they are not affected by weather and sunlight conditions. This study tries to extract collapsed bridges in the Pacific-coast of Tohoku, Japan, where the tsunamis inundated widely due to the Mw 9.0 earthquake on March 11, 2011. First, the positions of bridges were extracted using pre-event GIS data. Then, we attempted to detect collapsed or washed-away bridges by setting a proper threshold value on the SAR backscattering coefficient along the bridge's longitudinal axis using only a post-event high-resolution TerraSAR-X image. The results were compared with optical images and damage investigation reports, and then the effective use of SAR intensity image in the detection of bridge damage was demonstrated.*

1 INTRODUCTION

When an earthquake strikes, road networks are often fragmented by strong shaking or secondary effects, e.g. tsunami, landslide, liquefaction. In the 11 March 2011 Tohoku, Japan earthquake and associated tsunamis, the operational capabilities of field surveys were limited due to increased risk for emergency responders and the wide ranges of affected areas. For quick emergency response after an earthquake, the extraction of damaged areas at an early stage is very important to reduce casualties. At this point, the extraction of damages using Synthetic Aperture Radar (SAR) imagery, which can be acquired under all weather conditions both at daytime and night-time, is quite useful in an emergency response phase.

Due to remarkable improvements in radar sensors, high-resolution TerraSAR-X and COSMO-SkyMed SAR images are possible with ground resolution of 1 to 5 m, providing detailed surface information. The damage detection of urban areas using these high-resolution SAR images has become quite popular recently. Comparing the change in pre-event and post-event SAR intensity images, damage detection of buildings has been conducted several researchers [1-4]. Due to the side-looking nature of SAR, the layover of buildings and the multi-bounce of radar among the ground and buildings occur. If a building stands alone or faces to a wide street, the length of layover indicates the height of the building [5] and the status of its exterior wall facing to the radar illumination direction. Utilizing the change in the backscattering intensity within the layover area of an individual building, the damage situation of building exterior walls due to the 2011 Tohoku, Japan earthquake and tsunami was investigated [6].

Satellite images can also be applicable to detect damage situation of bridges. Shoji et al. [7] studied on the collapsed or washed-away girders and eroded approach-embankments of bridges due to the tsunamis caused by the 2011 Tohoku earthquake using the optical satellite images from Google Earth, and compared their results with the damage data from field surveys. Few studies have been reported on the damage assessment of bridge structures due to earthquakes or tsunamis, especially from SAR imagery. Furthermore, a pre-disaster image under the same acquisition condition as the post-disaster data does not often exist. Thus, this paper investigates the capability of SAR imagery in the bridge damage detection using only a post-event image.

In this study, the detection of collapsed or washed-away bridges was attempted by setting a proper threshold on the backscattering coefficient value along a bridge's longitudinal axis from a post-event TerraSAR-X (TSX) image. In order to verify the accuracy of this method, the detected results were compared with aerial optical images and field investigation reports.

2 STUDY AREA AND DATA USED

The study area was set in the Pacific coast of the Tohoku region, Japan, which was damaged severely by the 2011 Tohoku earthquake tsunami, as shown in Figure 1. Two TSX intensity images were taken on 12 March 2011 (20:43 UTC), about 1.5 days after the tsunami attack. The images were acquired in the StripMap mode with HH polarization. The incident angle at the centre of the image was about 33.2°, and the heading angle about 190.4°. The satellite path was descending with the right-look. The images were proved as the enhanced ellipsoid correction (EEC) products, and had been transformed into the pixel size of 1.25 m.

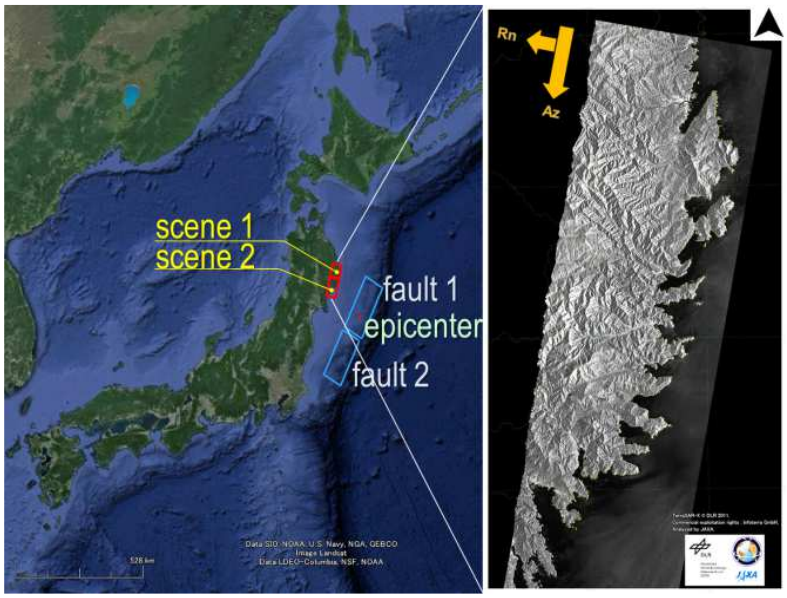

Figure 1: The study area along the Pacific coast of Tohoku, Japan and the post-event TerraSAR-X images taken on on March 12, 2011.

Two pre-processing steps were applied to the images before extracting collapsed bridges. First, the two TSX images were transformed to a sigma naught (σ_0) value, which represents the radar reflectivity per unit area in the ground range. An enhanced Lee filter was then applied to the original SAR images to reduce the speckle noise. To minimize any loss of information included in the intensity images, the window size of the filter was set as 5 × 5 pixels.

In order to extract the bridge positions and footprints, we used the GIS data provided by the Geospatial Information Authority of Japan [8]. As the reference data, a technical report by the National Institute for Land and Infrastructure Management was adopted [9]. Bridge damages were described by two categories which are “collapsed” and “survived.” For each bridge, the length, width, height, altitude, material information and the optical aerial photo are provided.

3 METHODOLOGY

In this study, the bridge that was collapsed, washed away or covered by water, was defined as “collapsed.” On the other hand, the situation that was no damage, cracked or covered with debris, was defined as “survived.” Twenty-two (22) collapsed bridges and 35 survived ones located in the TSX imaging area and also described in the reference data were focused as the targets. If a pedestrian bridge exists near the main bridge with the different IDs, they were treated as one bridge.

The footprints of bridges over water were automatically extracted using the pre-event GIS data. Specifically, the polygon surrounded by line data, which are the road edge and shoreline, was extracted as the target area. In the polygons, the footprints of bridges listed by the reference data were selected. Since the layover, double-bounce, and triple-bounce effects occur for bridge structures due to the side-looking geometry of SAR sensors as shown in Figure 2, we shifted the footprint of a bridge to the layover area calculated by Eq. (1).

$$L = h/\tan\theta. \quad (1)$$

where L is the layover length, h is the altitude of a bridge from the reference water level (T.P.), and θ is the incidence angle of radar.

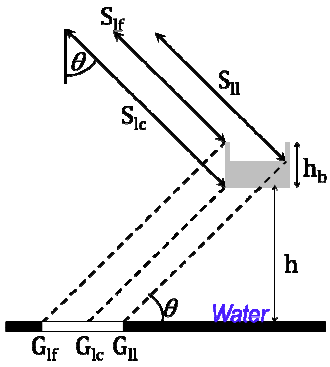

Figure 2: Layover area due to SAR imaging geometry

Then we attempted to detect bridge damage by a profile line method. For the each bridge crossing a river, three profile lines were drawn on the centre and both ends of the footprint after the shift, in order to extract the backscattering coefficients along the bridge's longitudinal axis from the left side to the right side in the image. Generally, the bigger backscattering intensity was observed along the bridge rail and the side-girder. On the other hand, a small intensity value was observed on the smooth road surface due to mirror reflection. Thus, we extracted the sigma naught value from the three profiles along left, centre, and right lines of the footprint. If a bridge is collapsed, a low sigma naught value of water will be extracted from parts of all the profiles.

First, the sigma naught value from each profile line was extracted and the minimum value, the average value (μ), and the standard deviation (σ) were calculated. If a girder or a rail is collapsed, all the values will be small whereas the high sigma naught is observed in the remaining part. The largest value of the three values was used for classification. If the value is lower than the threshold value, the bridge is classified as "collapsed."

An example for the bridges Nos.103 and 104 is shown in Figure 3. The three parameter values extracted from each profile is shown in Table 1. The minimum value of this bridge was extracted from the centre line as -56.3 dB, and used to compare with the threshold value.

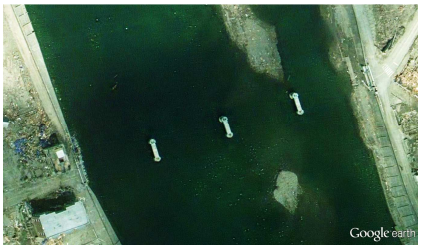

(a)

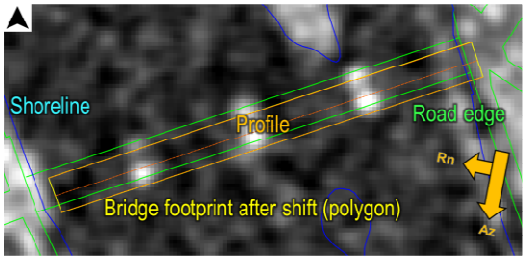

(b)

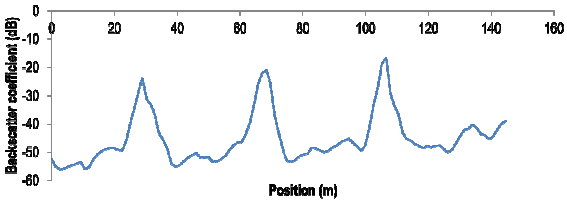

(c)

Figure 3: Optical image of Nos.103 & 104 bridges from Google Earth (a); shifting bridge footprint and drawing 3 profile lines (b); the profile graph along the centre line (c)

Second, the threshold value was assigned as the value which maximizes the kappa coefficient. The kappa coefficient shows agreement between the result from classification and the reference data. The kappa value ranges from -1.0 to 1.0, with 0.0 indicating no agreement equal to chance, and 1.0 indicating perfect agreement above chance. The kappa values are also divided into three classes: a value greater than 0.8 represents strong agreement, whereas the value between 0.4 and 0.8 represents moderate agreement, and a value below 0.4 represents poor agreement [10]. In this paper, we attempted to set 601 threshold values between -60.0 dB and 0.0 dB to calculate the kappa coefficients.

Sigma naught	left side	centre	right side
Min (dB)	-58.3	-56.3	-56.4
σ (dB)	7.0	8.8	4.9
μ (dB)	-46.4	-45.2	-46.7

Table 1: Statistics of the bridges Nos.103 and 104

4 RESULTS

Figure 4 (a) shows the number of bridges which were classified properly into two categories (black line) for different threshold values (horizontal axis). When the value in the ranges (-48.8 dB to -47.9 dB) and (-47.3 dB to -46.9 dB) were set as the threshold, the largest number of bridges (43 out of 57) were properly classified. Similarly, Figure 4 (b) and (c) focus the bridges whose lengths are longer than 50 m and longer than 100m. For the bridges over 50 m, the largest number of bridges (19 out of 22) were classified properly when the threshold was set in the range between -48.8 dB and -46.9 dB. For the bridges over 100 m, the largest number of bridges (8 out of 9) were classified properly when the threshold was set in the range between -52.5 dB and -50.3 dB or between -49.6 dB and -38.7 dB.

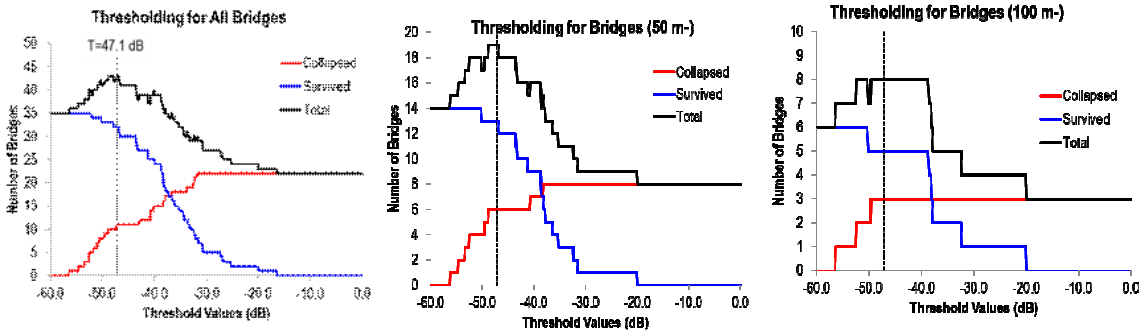

(a) All the 57 bridges (b) 22 bridges longer than 50 m (c) 9 bridges longer than 100 m

Figure 4: Number of bridges classified properly. (The dashed line is the threshold value)

Figure 5 (a) and (b) shows the overall accuracy and the kappa coefficient. The overall accuracy became the maximum value (75.4 %) for the values as mentioned above. On the other hand, the kappa coefficient became the maximum value (0.44; moderate agreement) when the threshold value in the range -47.3 dB to -46.9 dB (blue line). Thus, we set -47.1 dB as the threshold value. Table 2 exhibits the confusion matrix. For the bridges over 50 m (red line), the kappa value became 0.69 for the threshold between -48.8 dB and -46.9 dB. For the bridge over 100 m, it became 0.77 for the range -49.6 dB to -38.7 dB. The longer bridges show the better classification accuracy.

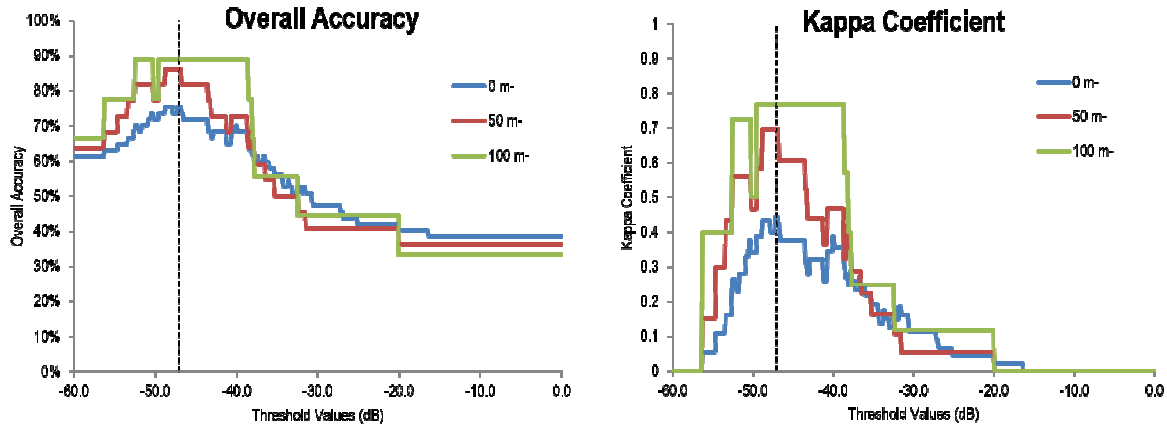

Figure 5: Overall accuracy and kappa coefficient for different threshold values

		Reference data			
Results from damage detection from TSX images		Collapsed	Survived	Total	User Accuracy
	Collapsed	10	2	12	83.3%
	Survived	12	33	45	73.3%
	Total	22	35	57	-
	Producer Accuracy	45.5%	94.3%	-	75.4%
	Kappa coefficient				0.44

Table 2: Confusion matrix when setting the threshold as -47.1 dB

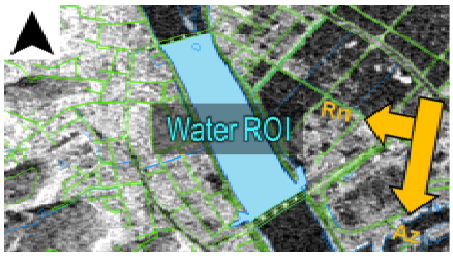

Figure 6: Extraction of the sigma naught (backscattering coefficient) value in a water area

Pixel count	61027 pixels
Mean	-49.4 dB
Standard deviation	3.8 dB
Max.	-16.8 dB
Min.	-62.1 dB

Table 3: Backscattering coefficient in a water area

In our assumption, the proper threshold value equals to the sigma naught for water areas. In order to compare between the threshold values and the backscattering coefficient of water, the region of interest (ROI) was set at the area surrounded by the shoreline of a river, as shown in Figure 6. We took statistics of the sigma naught value for water. The mean of backscattering coefficient in the water area (μ_w) was extracted from the ROI polygon as -49.4 dB, and the standard deviation (σ_w) was 3.8 dB as shown in Table 2. It is reasonable to set -

47.1 dB as the threshold value in this study since it within -49.4 ± 3.8 dB. Therefore, the threshold value should be set within $\mu_w \pm \sigma_w$ in other areas.

5 DISSCUSION AND CONCLUSIONS

This study carried out the profile line method in order to detect collapsed bridges due to the 2011 Tohoku, Japan earthquake tsunami using only a post-event SAR image and GIS data. The backscattering coefficient of typical survived and collapsed bridges were extracted along the bridge's longitudinal axis. In order to classify the bridges, the proper threshold value which optimized the kappa coefficient was considered.

The best classification was performed when -47.1 dB was set as the threshold value, and 10 collapsed bridges out of 22, 33 survived bridges out of 35 were classified properly. For the bridges longer than 50 m, 6 collapsed bridges out of 8 and 13 survived bridges out of 14 were properly classified. At the same time, the overall accuracy was 86.4 % and the kappa coefficient was 0.70. Correspondingly, for the bridges longer than 100 m, all collapsed bridges out of three and five survived bridges out of five were properly classified. At the same time, the overall accuracy was 88.9 % and the kappa coefficient was 0.77. For the short bridges, the backscattering coefficient value of water could not be extracted due to the resolution, and thus it was difficult to classify between collapsed and survived.

In this study, we focused on the bridges over river water. Regarding bridges over ground, adopting the standard deviation and texture features can be considered. For instance, if a bridge is collapsed, the standard deviations of profile lines become large and the texture gets smooth. But we still need to accumulate validation data until a solid conclusion is drawn.

ACKNOWLEDGEMENTS

The TerraSAR-X image used in this study is property of the German Aerospace Center (DLR) and was licensed to Chiba University. This study was financially supported by the Grant-in-Aid for Scientific Research (project numbers: 15K16305, 24241059), and the Core Research for Evolutional Science and Technology (CREST) program by the Japan Science and Technology Agency (JST), "Establishing the most advanced disaster reduction management system by fusion of real-time disaster simulation and big data assimilation."

REFERENCES

[1] Brunner, D., Lemoine, G., and Bruzzone, L., "Earthquake damage assessment of buildings using VHR optical and SAR imagery," IEEE Transactions on Geoscience and Remote Sensing, 48(5), 2403-2420 (2010).

[2] Miura, H. and Midorikawa, S., "Preliminary Analysis for Building Damage Detection from High-Resolution SAR Images of the 2010 Haiti Earthquake," Joint Conference Proceedings of 9th International Conference on Urban Earthquake Engineering and 4th Asia Conference on Earthquake Engineering, Paper No.01-212 (2012).

[3] Uprety, P., Yamazaki, F., Dell'Acqua, F., "Damage detection using high-resolution SAR imagery in the 2009 L'Aquila, Italy, earthquake," Earthqake Spectra, 29, 1521-1535 (2013).

[4] Liu, W., Yamazaki, F., Gokon, H., and Koshimura, S., "Extraction of Tsunami-Flooded Areas and Damaged Buildings in the 2011 Tohoku-Oki Earthquake from TerraSAR-X Intensity Images," Earthquake Spectra, 29(S1), S183-S200 (2013).

[5] Liu, W., Yamazaki, F., "Building height detection from high-resolution TerraSAR-X imagery and GIS data," Proceedings of 2013 Joint Urban Remote Sensing Event, Sao Paulo, Brazil, CD-ROM, 33-36 (2013).
[6] Yamazaki, F., Liu, W., "Urban change monitoring: multi-temporal SAR images," Encyclopedia of Earthquake Engineering, DOI 10.1007/978-3-642-36197-5_227-1, Springer-Verlag Berlin Heidelberg, (2014).
[7] Shoji, G., Takahashi, K., Nakamura, T., 2012, "Tsunami damage assessment on bridge structures subjected to the 2011 off the Pacific coast of Tohoku earthquake tsunami," Journal of JAEE, Vol. 12, No. 6, pp. 104-191 (2014). in Japanese.
[8] Geospatial Information Authority of Japan. GSI Maps. http://maps.gsi.go.jp/. Accessed on February 7, 2016.
[9] Tamakoshi, T., Yokoi, Y., Kawai, S., "Damage to road bridges by the 2011 off the Pacific coast of Tohoku earthquake and tsunami," Technical Note of National Institute for Land and Infrastructure Management No.843, 23-110 (2015). in Japanese.
[10] Congalton, R. G., "A review of assessing the accuracy of classifications of remotely sensed data, " Remote Sensing of Environment 37, 35-46 (1991).